AD_____

GRANT NUMBER: DAMD17-94-J-4377

TITLE: Classification of Microcalcifications of the Diagnosis of
Breast Cancer Using Artificial Neural Networks

PRINCIPAL INVESTIGATOR: Yuzheng C. Wu, Ph.D.

CONTRACTING ORGANIZATION: Georgetown University
                           Washington, DC 20057

REPORT DATE: September 1996

TYPE OF REPORT: Annual

DTIC QUALITY INSPECTED 2

PREPARED FOR: Commander
               U.S. Army Medical Research and Materiel Command
               Fort Detrick, Frederick, MD 21702-5012

DISTRIBUTION STATEMENT: Approved for public release;
                         distribution unlimited

The views, opinions and/or findings contained in this report are
those of the author(s) and should not be construed as an official
Department of the Army position, policy or decision unless so
designated by other documentation.

19970610 027

REPORT DOCUMENTATION PAGE

Public reporting burden for this collection of information is estimated to average 1 hour per response, including the time for reviewing instructions, searching existing data sources, gathering and maintaining the data needed, and completing and reviewing the collection of information. Send comments regarding this burden estimate or any other aspect of this collection of information, including suggestions for reducing this burden, to Washington Headquarters Services, Directorate for Information Operations and Reports, 1215 Jefferson Davis Highway, Suite 1204, Arlington, VA 22202-4302, and to the Office of Management and Budget, Paperwork Reduction Project (0704-0188), Washington, DC 20503.

1. AGENCY USE ONLY (Leave blank)	2. REPORT DATE	3. REPORT TYPE AND DATES COVERED
	September 1996	Annual (1 Sep 95 – 31 Aug 96)

4. TITLE AND SUBTITLE
Classification of Microcalifications of the Diagnosis of Breast Cancer Using Artificial Neural Networks

5. FUNDING NUMBERS
DAMD17-94-J-4377

6. AUTHOR(S)
Yuzheng C. Wu, Ph.D.

7. PERFORMING ORGANIZATION NAME(S) AND ADDRESS(ES)
Georgetown University
Washington, DC 20057

8. PERFORMING ORGANIZATION REPORT NUMBER

9. SPONSORING/MONITORING AGENCY NAME(S) AND ADDRESS(ES)
Commander
U.S. Army Medical Research and Materiel Command,
Fort Detrick, Frederick, MD 21702-5012

10. SPONSORING/MONITORING AGENCY REPORT NUMBER

11. SUPPLEMENTARY NOTES

12a. DISTRIBUTION/AVAILABILITY STATEMENT
Approved for public release;
distribution unlimited

12b. DISTRIBUTION CODE

13. ABSTRACT (Maximum 200 words)

Early detection of breast cancer depends on the accurate classification of microcalcifications. We have developed a computer vision system that can classify microcalcifications objectively and consistently to aid radiologists in the diagnosis of breast cancer.

A convolution neural network (CNN) was employed to classify benign and malignant microcalcifications in the radiographs of pathological specimen that were digitized at a high resolution of 21 µm x 21 µm. The CNN achieved an A_z value of 0.90 in classifying clusters of microcalcifications associated with benign and malignant processes. An automated image feature extraction technique and feature-based neural network optimized with generic algorithms were applied to clinical mammograms as an alternative approach to the classification. The neural network system performed better than a radiologist in distinguishing between benign and subtle malignant clusters.

The classification of microcalcifications for the diagnosis of breast cancer was achieved at a high level in our computer vision system that consists of high resolution digitization of mammograms and neural network systems. The classification of microcalcifications can be used to help reducing unnecessary biopsies in diagnosis of breast cancer.

14. SUBJECT TERMS
Breast Cancer

15. NUMBER OF PAGES
30

16. PRICE CODE

17. SECURITY CLASSIFICATION OF REPORT	18. SECURITY CLASSIFICATION OF THIS PAGE	19. SECURITY CLASSIFICATION OF ABSTRACT	20. LIMITATION OF ABSTRACT
Unclassified	Unclassified	Unclassified	Unlimited

NSN 7540-01-280-5500

Standard Form 298 (Rev. 2-89)
Prescribed by ANSI Std. Z39-18
298-102

GENERAL INSTRUCTIONS FOR COMPLETING SF 298

The Report Documentation Page (RDP) is used in announcing and cataloging reports. It is important that this information be consistent with the rest of the report, particularly the cover and title page. Instructions for filling in each block of the form follow. It is important to *stay within the lines* to meet *optical scanning requirements*.

Block 1. Agency Use Only *(Leave blank)*.

Block 2. Report Date. Full publication date including day, month, and year, if available (e.g. 1 Jan 88). Must cite at least the year.

Block 3. Type of Report and Dates Covered. State whether report is interim, final, etc. If applicable, enter inclusive report dates (e.g. 10 Jun 87 - 30 Jun 88).

Block 4. Title and Subtitle. A title is taken from the part of the report that provides the most meaningful and complete information. When a report is prepared in more than one volume, repeat the primary title, add volume number, and include subtitle for the specific volume. On classified documents enter the title classification in parentheses.

Block 5. Funding Numbers. To include contract and grant numbers; may include program element number(s), project number(s), task number(s), and work unit number(s). Use the following labels:

C	-	Contract	**PR** - Project
G	-	Grant	**TA** - Task
PE	-	Program Element	**WU** - Work Unit Accession No.

Block 6. Author(s). Name(s) of person(s) responsible for writing the report, performing the research, or credited with the content of the report. If editor or compiler, this should follow the name(s).

Block 7. Performing Organization Name(s) and Address(es). Self-explanatory.

Block 8. Performing Organization Report Number. Enter the unique alphanumeric report number(s) assigned by the organization performing the report.

Block 9. Sponsoring/Monitoring Agency Name(s) and Address(es). Self-explanatory.

Block 10. Sponsoring/Monitoring Agency Report Number. *(If known)*

Block 11. Supplementary Notes. Enter information not included elsewhere such as: Prepared in cooperation with...; Trans. of...; To be published in.... When a report is revised, include a statement whether the new report supersedes or supplements the older report.

Block 12a. Distribution/Availability Statement. Denotes public availability or limitations. Cite any availability to the public. Enter additional limitations or special markings in all capitals (e.g. NOFORN, REL, ITAR).

DOD	-	See DoDD 5230.24, "Distribution Statements on Technical Documents."
DOE	-	See authorities.
NASA	-	See Handbook NHB 2200.2.
NTIS	-	Leave blank.

Block 12b. Distribution Code.

DOD	-	Leave blank.
DOE	-	Enter DOE distribution categories from the Standard Distribution for Unclassified Scientific and Technical Reports.
NASA	-	Leave blank.
NTIS	-	Leave blank.

Block 13. Abstract. Include a brief *(Maximum 200 words)* factual summary of the most significant information contained in the report.

Block 14. Subject Terms. Keywords or phrases identifying major subjects in the report.

Block 15. Number of Pages. Enter the total number of pages.

Block 16. Price Code. Enter appropriate price code *(NTIS only)*.

Blocks 17. - 19. Security Classifications. Self-explanatory. Enter U.S. Security Classification in accordance with U.S. Security Regulations (i.e., UNCLASSIFIED). If form contains classified information, stamp classification on the top and bottom of the page.

Block 20. Limitation of Abstract. This block must be completed to assign a limitation to the abstract. Enter either UL (unlimited) or SAR (same as report). An entry in this block is necessary if the abstract is to be limited. If blank, the abstract is assumed to be unlimited.

FOREWORD

Opinions, interpretations, conclusions and recommendations are those of the author and are not necessarily endorsed by the US Army.

_____ Where copyrighted material is quoted, permission has been obtained to use such material.

_____ Where material from documents designated for limited distribution is quoted, permission has been obtained to use the material.

__✓__ Citations of commercial organizations and trade names in this report do not constitute an official Department of Army endorsement or approval of the products or services of these organizations.

_____ In conducting research using animals, the investigator(s) adhered to the "Guide for the Care and Use of Laboratory Animals," prepared by the Committee on Care and Use of Laboratory Animals of the Institute of Laboratory Resources, National Research Council (NIH Publication No. 86-23, Revised 1985).

_____ For the protection of human subjects, the investigator(s) adhered to policies of applicable Federal Law 45 CFR 46.

_____ In conducting research utilizing recombinant DNA technology, the investigator(s) adhered to current guidelines promulgated by the National Institutes of Health.

_____ In the conduct of research utilizing recombinant DNA, the investigator(s) adhered to the NIH Guidelines for Research Involving Recombinant DNA Molecules.

_____ In the conduct of research involving hazardous organisms, the investigator(s) adhered to the CDC-NIH Guide for Biosafety in Microbiological and Biomedical Laboratories.

PI - Signature   Date
11/24/86

3

Table of Contents

Introduction

Breast cancer is one of the leading causes of death among women. However, there is clear evidence that early diagnosis and subsequent treatment can significantly improve the chance of survival for patients with breast cancer.[1-4]

Mammography has become one of the major diagnostic procedures with a proven capability for detecting early-stage, clinically occult breast cancers.[5-8] However, breast cancers in their early stage are small and frequently their radiographic appearance differs only subtly from that of normal tissue or benign abnormalities. Because of this subtlety, the potential for misclassification by radiologists is substantial. Only 10-30% of cases that have mammographically suspicious findings and are subjected to biopsy prove to be malignant.[9] On the other hand, approximately 10-30% of patients with breast cancer are misdiagnosed by mammography (have the cancer missed or not detected on their mammograms).[10-14]

Besides the subtle nature of radiographic lesions associated with breast cancer, many errors in radiological diagnoses can be attributed to human factors such as subjective or varying decision criteria, distraction by other image features, and simple oversight.[15-17] Studies suggest that these errors may occur even with experienced radiologists.[18,19] These errors may be reduced by the use of automated detection schemes that can locate and classify possible lesions, thereby alerting the radiologist to examine these areas with particular caution. Moreover, the automated detection schemes can serve as a "second radiologist", similar to the double reading by two radiologists that is commonly practiced in diagnostic radiology to increase diagnostic efficacy.

Microcalcifications are commonly considered to be important signs of breast cancer. It has been reported that 30-50% of breast cancers detected radiographically demonstrate microcalcifications on mammograms.[20-25] Up to 90% of cases of ductal carcinoma in situ present with microcalcifications.[26] The correlation between the presence of microcalcifications and the presence of breast cancer suggests that accurate detection of microcalcifications will improve the efficacy of mammography as a diagnostic procedure.

Microcalcifications occur in malignant and benign conditions. Some microcalcifications are characteristically benign or are associated with a benign process. For example, calcified fibroadenomas have a typical "popcorn" configuration appearing coarse and solitary. Milk of calcium demonstrates sedimentation.[27] Vascular calcifications have a tram track appearance, typical of vascular calcifications seen in other areas of the body. Dermal calcifications tend to be smooth and round with lucent centers. Secretory calcifications are thick, smooth, cigar-shaped, and usually non-branching. Features supporting benignity include uniform size and density of the calcium flecks, as is seen in sclerosing adenosis.[28] Furthermore, benign microcalcifications tend to be uniformly dense or scattered, without a segmental or linear distribution.[29]

Some microcalcifications associated with malignancy have a typically granular or linear appearance. They usually occur in clusters consisting of greater than 15 particles.[30] The particle size is small (less than 1 mm) and the shape is irregular.[31] Some clusters of microcalcifications have neither the typically benign nor typically malignant configurations

described above. These "indeterminate" microcalcifications present a significant diagnostic problem and require careful analysis.

The number of microcalcifications per cm^2 has been shown to be the most important predictor of malignancy, with clusters consisting of less than 10 microcalcifications per cm^2 having a high chance of benignity. Clusters consisting of microcalcifications numbering greater than 15 per cm^2 have a higher chance of malignancy.[32]

The task of detection and classification of microcalcifications for the diagnosis of breast cancer is a difficult one. The inability to correctly predict cancer is not only due to the overlap in appearance between microcalcifications associated with benign and malignant conditions, dense breasts, improper technical factors or simple oversight by radiologists may contribute to the failure to detect microcalcifications. Differing levels of confidence and training among interpreting radiologists may lead to inconsistent recommendations for management.

Radiologists classify breast microcalcifications into one of three groups: benign, likely malignant, and indeterminate. Most patients with indeterminate types of calcifications undergo a breast biopsy to exclude cancer. Any method that would correctly classify benign types of calcifications previously considered indeterminate would decrease the frequency of biopsy and therefore the cost of detection of breast cancer.

Several investigators have been developing computer programs for the automated detection of microcalcifications on mammograms.[33-36] Chan *et al.* showed that the computer program can detect subtle microcalcifications that may be missed by radiologists, indicating that it is a promising approach to the automated detection of microcalcifications.[37] More recently, Wu *et al.* applied an artificial neural network (ANN) to detect microcalcifications.[38] The ANN, trained by using the power spectrum of regions of interests (ROI) containing microcalcifications, was able to eliminate 50% of false-positive detections of a rule-based scheme[37,39] while preserving more than 95% of the true-positive detections. The neural network achieved an A_z value of 0.85 for the detection of clustered microcalcifications. Several other computer schemes for detection of microcalcifications were also reported by Astley *et al.*,[40] based on likelihood estimators, by Grimaud *et al.*,[41] using mathematical morphology tools, and by Karssemeijer,[42] using a stochastic method based on Bayesian decision theory.

As stated earlier, microcalcifications can be associated with either benign or malignant processes. It is important to distinguish different types of microcalcifications after they have been identified by a detection scheme. Accurate classification of microcalcifications into benign and malignant groups would help improve the sensitivity of the diagnosis as well as reduce the number of unnecessary biopsies.

As the first step in the process of developing an automated computer scheme for classification of microcalcifications, a neural network system was developed to classify microcalcifications in the radiographs of biopsy specimens. Classification of microcalcifications in radiographs of biopsy specimens is an "idealized" situation.

In biopsy specimens, underlying tissue around microcalcifications is less than that present in normal mammograms. Therefore, the scatter radiation recorded on films is reduced, resulting in improved contrast. Higher dose and geometrical magnification can also be used to obtain radiographs of biopsy specimens as compared with regular mammograms. Less magnification results in less geometrical unsharpness. Higher exposure can be used to achieve greater signal to noise ratio and thereby improve image quality of radiographs.

Therefore, microcalcifications in the radiographs of biopsy specimens are more clearly represented than those in regular mammograms. After we can successfully apply our algorithm to classify microcalcifications in radiographs of specimens, we will make necessary adjustments to apply the algorithm to the regular mammograms.

In recent years, rapid progress of research on artificial neural networks (ANN)[43] has been reported extensively in the field of computer science and many applied fields. Neural networks address detection, classification, and decision-making problems not by pre-specified "conventional" algorithms, but rather by "learning" from examples presented repeatedly. The popularity of neural networks is primarily due to their apparent ability to make decisions and draw conclusions when presented with complex, noisy, or partial information and to adapt their behavior to the properties of the training data. Neural networks are capable of parallel-processing a large amount of information simultaneously and have been shown[44,45] to be a useful tool for pattern recognition in fields where conventional algorithmic approaches and rule-based expert systems may not be successful.

Body of Report

METHODS

Algorithms for classification of microcalcifications have been developed in two stages. First, a convolution neural network based method was developed to classify microcalcifications using radiographs of pathological specimen. Second, an image feature based method was developed to classify microcalcifications using real mammograms. The image features used and optimal structure of the backpropagation neural network were determined by using genetic algorithm.

Classification of microcalcifications in pathological specimen

The overall approach for the classification of microcalcifications using a CNN system is shown in Figure 1. The radiographs of pathological specimen are digitized by a high resolution digitizer. Regions of interest (ROI) containing microcalcifications are manually selected. These ROIs are preprocessed and used as input to the CNN system. Finally, the classification results are examined by the ROC analysis.
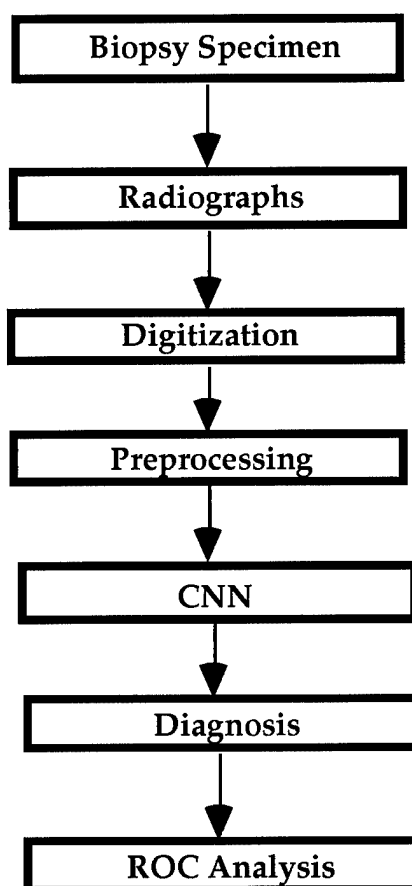

Figure 1.   Overall approach for the classification of microcalcifications using CNN.

The classification of microcalcifications is based primarily on the fact that microcalcifications associated with malignant processes generally have more irregular shapes with fuzzy and spiculated boundaries and are less uniform in density and size. They are usually grouped into multi-particle clusters. The microcalcifications associated with benign processes, on the other hand, usually tend to have smoother and well-defined boundaries, rounded shape, and uniform densities and sizes. The neural network system will be trained to recognize the characteristics of each type of microcalcifications.

The CNN is based on the network structure of Fukushima's Neocognitron[46] which is designed to simulate the vision of vertebrate animals. The structure of CNN used in this study resembles a simplified Neocognitron. A two-dimensional convolution operation from the input layer to the hidden layer is employed to simulate radiologists' viewing of a suspected area. The CNN has the ability to process and recognize two dimensional image patterns and has been shown to be an effective tool in image processing and pattern recognition.[47-49]

Acquisition of Mammograms

The selected radiographs of breast biopsy specimen are digitized with an image resolution of 21μm x 21μm per pixel by a CCD camera digitizer (DBA Systems Inc.). With high resolution digitization, the morphological information of microcalcifications can be preserved, which enables the neural network system to differentiate different types of microcalcifications on the basis of their geometrical shapes and density patterns. Figure 2(a) shows a cluster of microcalcifications in original radiographs of pathological specimen. Shown in Figure 2(b) are clustered microcalcifications after being digitized with the high resolution digitizer. The shapes and density patterns of the microcalcifications are better defined in Fig. 2(b) than those shown in Fig. 2(a).

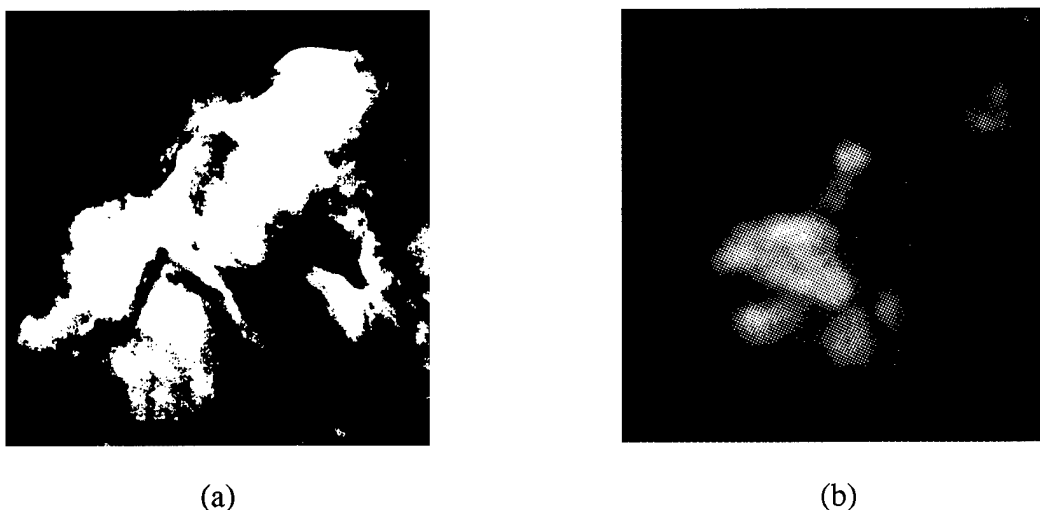(a)   (b)

Figure 2.   Microcalcifications shown in an original radiograph of pathological specimen (a) and shown in a radiograph digitized with a high resolution (21 μm × 21 μm) digitizer (b).

Convolution Neural Network

The structure of the CNN[47] is shown in Figure 3. The input to the CNN are ROIs of matrix size of 64×64 pixels, containing benign or malignant type of microcalcifications. Only one hidden layer is used in this study. The connections between input and hidden layer are grouped into seven different kernels based on the structure of Fukushima's Neocognitron.[46,50] There are two output units in the output layer, with each unit corresponding to a benign or malignant class of microcalcifications. The hidden layer and the output layers are fully connected.

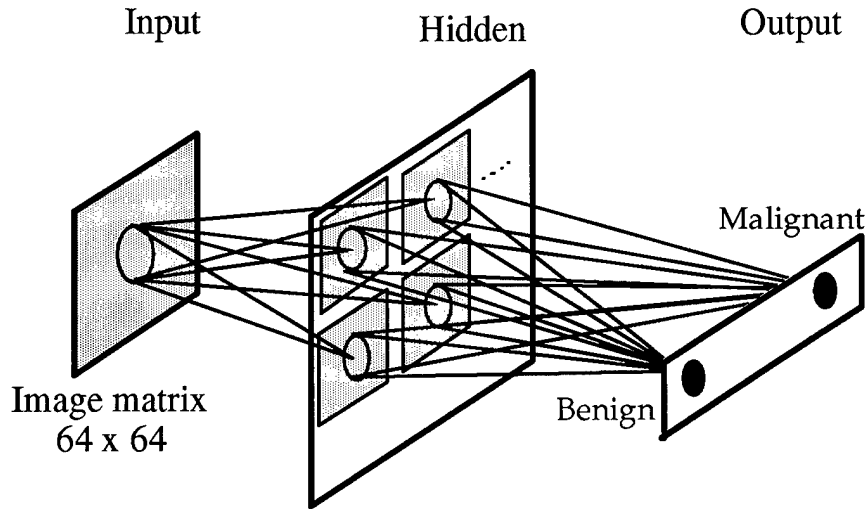Input   Hidden   Output

Figure 3.   Structure of a convolution neural network used for the classification of
            microcalcifications.

The training algorithm of the CNN is similar to that of a backpropagation neural network, in which backpropagation and the generalized delta rule are used in the training process.[51] The input signals are now two dimensional images. The weights are all arranged in the convolution kernels. In the feed-forward propagation, the output of lth layer are first convoluted with weight filters. The sum of the convolution is then added by a bias term to form the net input to the next layer.

$$N_q^{l+1}(x,y) = \sum_{p=1}^{P^l} [O_p^l * W_{p,q}^l]_{(x,y)} + b_q^{l+1} \tag{1}$$

where $N_p^{l+1}(x,y)$ is the net input to the unit (x,y) in layer $l+1$, $O_p^l(x,y)$ is the output of the unit in layer l, $W_{p,q}^l(x,y)$ is a weight kernel, and b_q^{l+1} is a bias term in layer $l+1$. In the notation, layer number $l = (1, 2, ..., L)$, cluster number in the lth layer p = $(1, 2, ..., P^l)$, and

cluster number in the $(l+1)$th layer q = (1, 2, ..., P^{l+1}). Note that $*$ denotes discrete convolution,

$$[O_p^l * W_{p,q}^l]_{(x,y)} = \sum_i \sum_j (O_p^l(i,j) \cdot W_{p,q}^l(i-x, j-y)) . \qquad [2]$$

We can then rewrite equation [1] as

$$O_q^{l+1}(x,y) = f(N_q^{l+1}(x,y)), \qquad [3]$$

where f is the activation function

$$f(x) = \frac{1}{1 + \exp(-x)} . \qquad [4]$$

In the error backpropagation, the weights are modified, similar to that in Eqn.[2], as the following,

$$\Delta W_{p,q}^l(n+1) = \eta(d_q^{l+1} * O_p^l) + \alpha \Delta W_{p,q}^l(n), \qquad [5]$$

to minimize the error function,

$$E = \frac{1}{2} \sum (T(x,y) - O_1^L(x,y))^2 , \qquad [6]$$

where $T(x,y)$ is the target output.

In the training process of the CNN, each image block is rotated and reflected such that the number of training data are increased eight fold. The rotation and reflection represent different orientations of microcalcifications in mammograms. The training with additional orientation can effectively make the CNN rotational invariant.

Classification of microcalcifications in real mammograms

An alternative approach was employed to classify microcalcifications of in clinical mammograms. Microcalcifications can be characterized by a number of quantitative variables describing the underlying key features of a suspicious region such as the size, shape, and number of microcalcifications in a cluster. These features are calculated by an automated extraction scheme for each of the selected regions. The features are then used as input to a backpropagation neural network to make a decision regarding the probability of malignancy of a selected region. The initial selection of image features set was a rough estimation that may include redundant and non-discriminant features. A genetic algorithm was employed to select an optimal image feature set from the initial feature set and select an optimized structure of the neural network for the optimal input features. Finally, the performance of optimized neural network is evaluated using the selected sub-features. The performance of neural network is then compared with that of radiologists in classifying the clusters of microcalcifications.

A selected region is a 256×256 matrix from a mammogram that is digitized at 50 microns per pixel with a Lumisys scanner. Figure 4 shows two regions of interest (ROI) selected from original mammograms: (a) benign and (b) malignant. The background trend in a selected region is eliminated by an adaptive trend correction technique. The trend-corrected image is then binarized by taking the top level of 32 quantization levels. A series of pre-processing techniques that include open and dilation operations, logic AND, and labeling operation are applied to the binary image to eliminate artifacts while preserving the original shapes of microcalcifications. Image features are extracted based on the pre-processed image and two morphologically filtered images. Nineteen image features are extracted for each cluster of microcalcifications characterizing the size, number of microcalcification in the cluster, and shape.
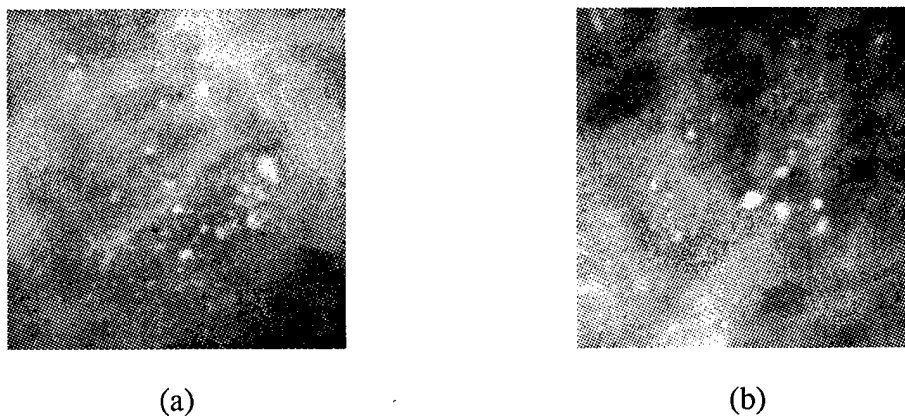

(a)   (b)

Figure 4   Two ROIs of size 256 x 256 selected from original mammgrams: (a) benign and (b) malignant

Pre-Processing

The pre-processing algorithm is demonstrated in Figure 5. The purpose of pre-processing is to obtain a binary image of microcalcifications. The pixels representing microcalcifications have values of one and the rest have values of zero. We need only binary image because image features we use are not based on density but rather based on only size, shape, clustering, and number of microcalcifications in a cluster.
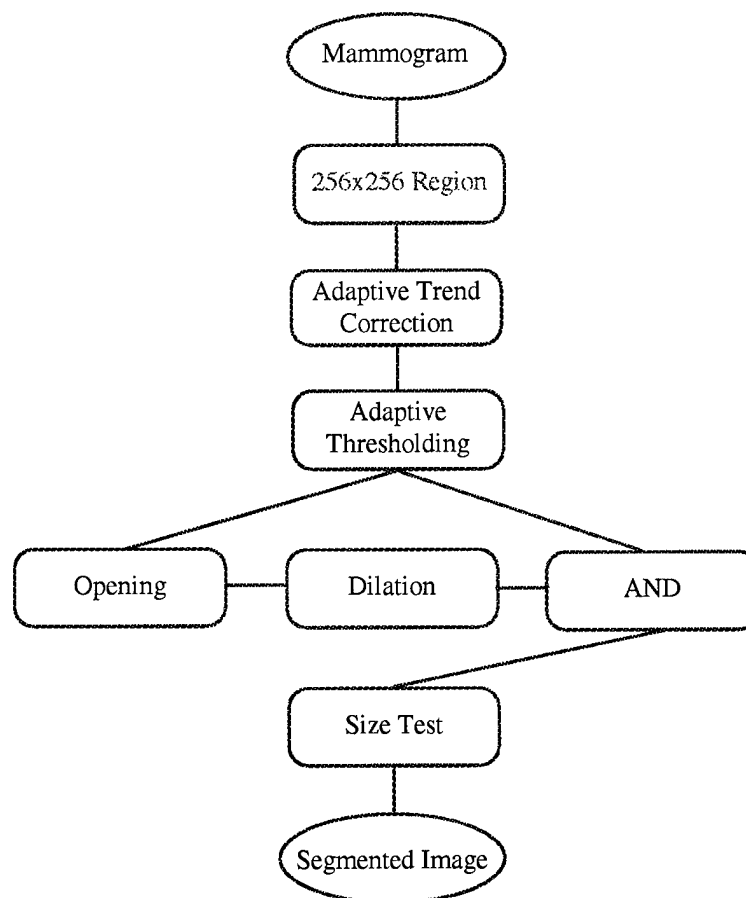

Figure 5 Pre-Processing of Selected Region of a Mammogram

a. Adaptive background trend correction

A average filter of kernel size of 23 × 23 pixels is used to remove the background trend in a selected region. At each pixel in the selected region, an average value is calculated for the surrounding 23 × 23 pixels and subtracted from the original pixel value. This process is repeated for all the pixels in the selected region. The adaptive technique is used to isolate microcalcifications from their immediate surroundings rather than from a different region that may have a different density level. As long as the sizes of microcalcifications remain small and microcalcifications are not clustered too close to each other, this method will be able to preserve the original shapes of microcalcifications. The kernel size of 23 pixels is equivalent

of approximately 1.2mm. Therefore, microcalcifications that are larger than 1.2mm in size are eliminated by the background correction process.

b. Adaptive thresholding

After background correction, a threshold is applied to the image such that only 2048 pixels of highest intensity (pixel value) are kept (assigned pixel value 1) and the rest pixels are assigned pixel values of 0. The number of pixels that are kept after thresholding is determined empirically that the sizes of microcalcifications in the threshold image are similar to those in the original image.

c. Opening operation

A morphological Opening operation with 3 x 3 kernel size is applied to the binary image to remove line artifact. The Opening is a combination of an erosion followed by a dilation.

d. Dilation

A morphological Dilation operation is applied after the OPEN operation to fill in the small holes near the boundary of an object.

e. AND operation

To preserve the shape of microcalcifications, an AND operation between the original binary image and the image after dilation is performed.

f. Labeling

A labeling process is applied after the AND operation to eliminate small objects that still remain in the image that are less than 5 pixels in size. Any object that is that small is unlikely to be an microcalcification.

Image Feature Extraction

Three images are used in feature extraction. The three images are: Image1, the preprocessed image; Image2, dilation of Image1 by a 5×5 kernel; Image3, dilation of Image1 by a 25×25 kernel. The process is demonstrated in Figure 6.

1. Number of microcalcifications N from Image1

2. Area (number of pixels) in Image1 S1

3. Area (number of pixels) in Image2 S2

4. Area (number of pixels) in Image3 S3

5. (S2-S1)/N, a measure of average number of irregular pixels

6. (S3-S1)/N, a measure of average distance between microcalcifications in a cluster

7. (S2-S1), total number of irregular pixels

8. (S3-S1), a measure of average distance between microcalcifications in a cluster

9. V1, size of the largest microcalcification in Image1 - size of average microcalcification in Image1

10. V2, size of the average microcalcification in Image1 - size of the smallest microcalcification in Image1

11. V3, size of the largest microcalcification in Image1

12. V4, size of average microcalcification in Image1

13. V5, size of smallest microcalcification in Image1

14. E1, ellipticity of the largest microcalcification on Image1

15. WAE, weighted average ellipticity of microcalcifications on Image1

16. A_x, length of semi-major axes of the fitted ellipse of a cluster on Image1

17. B_x, length of semi-minor axes of the fitted ellipse of a cluster on Image1

18. A_x / B_x

19. $A_x \times B_x$

A total of 19 image features are extracted for candidate cluster and used as input to a backpropagation neural network.
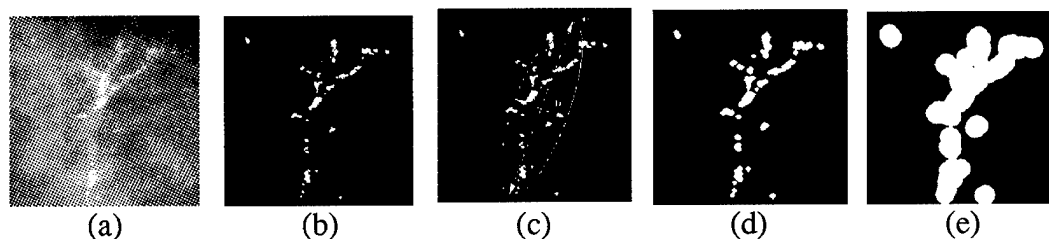

(a)   (b)   (c)   (d)   (e)

Figure 6   (a) Original gray scale image, (b) Binary image, (c) Best-fit ellipse and its semi-major axis A_x and semi-minor axis B_x, (d) Dilation with 5×5 kernel, and (e) Dilation with 25×25 kernel.

Genetic Algorithms

Genetic algorithms are directly modeled after biological systems and behavior. All the values of a structure represent the neural network characteristics that uniquely define a candidate solution in the space of possible solutions. Utilizing genetic algorithms, the Genetic Supervisor evolves successor populations, or generations, from a limited population of initial candidate solutions. It does this by treating the inclusion or exclusion of each column of data in the full Input column set as features; the number of layers and the number of neurons per layers as features; and the control parameters of each neural network as features.

These features are then varied in each new generation with the resulting structure evaluated in terms of neural network fitness. Each structure in the generation is evaluated and judged by either the lowest RMS Error achieved after a fixed number of epochs or by the number of epochs taken to achieve a minimum point in RMNS Error. These two measures represent neural networks that train to minimal error or neural networks which train with minimal epochs. These criteria can be applied to the set of training cases or the set of test cases.

If the structure representing a neural network successfully meets the fitness criteria selected, then the values of its features will be retained and bred with other structures. For each generation, the Genetic Supervisor generates a population of structures in on of two ways. All the structures of an initial generation and a certain number of structures in subsequent generations are created with features set to random values constrained within specified limits. Subsequent generations are created by cross-breeding the strings of successful structures or occasional mutations of randomly selected features of successful structures. Some or many of the weakest structure may be culled, these are replaced with new structures.

Through this evolution-like process, an optimal neural network can be developed. Note, however, that this process requires the training of many versions of the neural network to determine an optimal one; for neural network models that have large network configurations or have large data sets this can be a lengthy process – but so can biological evolution!

A system consisting of a Backpropagation neural network and a Genetic Supervisor is developed to classify the extracted image features. The Genetic Supervisor attempts to select the best subset of image features from the provided input set, configure the best neural network structure, and adjust the parameters of the network for optimum performance. The performance of the neural network system is evaluated by ROC analysis.

Reduction of Patient Call Backs

A third set of images will be selected at GUMC which are images of patients that are called back after screening exam to follow up. A majority of the called back patients are benign. The objective is to reduce the number of call back patients are definitely benign and therefore reduce the overall cost of breast cancer diagnosis practice.
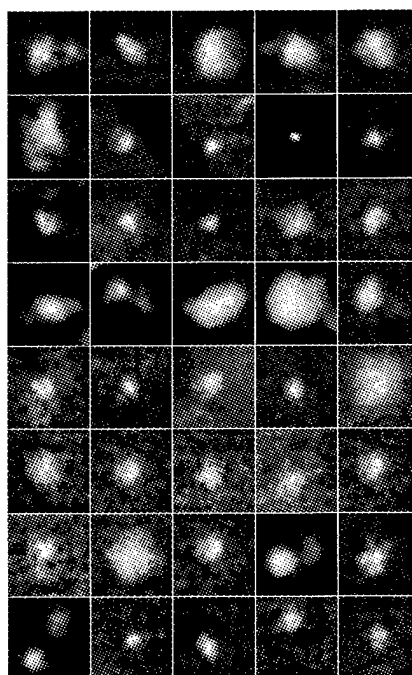
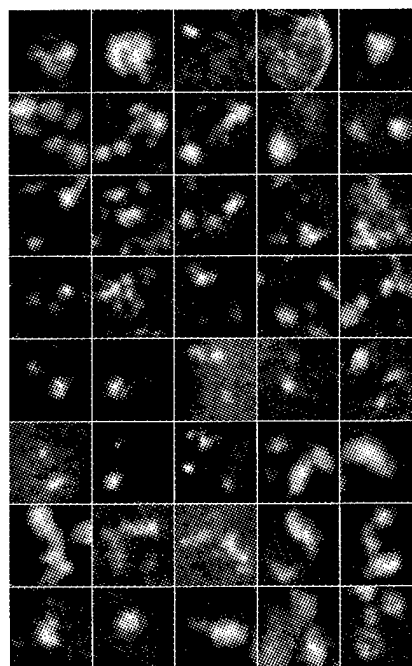**Database**

Pathological Specimen Images

Eighty regions of interest (ROI) that contain clustered microcalcifications (40 benign and 40 malignant) are selected from 60 digitized radiographs of pathological specimen in this study. Figure 7 shows all of the 80 ROIs selected in the database. There are substantial variations in size among benign or malignant microcalcifications. The information concerning the classification of microcalcifications ("truth") are obtained from the results of biopsy examination. Background trend correction is employed to remove the non-uniform background structure in different ROIs.

Clinical Mammograms

Two sets of clinical mammograms were collected. The first set contains 70 cases of clusters of microcalcifications and the second set contains 62 cases of microcalcifications. The two sets cases were selected from two different sources of medical institutions. The microcalcifications in both sets were rated subtle by radiologists. The diagnostic truth of all of the cases in the selected sets had been verified by biopsy.

(a)

(b)

Figure 7   Database for the training and testing of the CNN; (a) 40 ROIs containing benign clustered microcalcifications and (b) 40 ROIs containing malignant clustered microcalcifications.

RESULTS

images of pathological Specimen

Jackknife Method

A jackknife method was employed to evaluate the performance of the CNN. In the jackknife method, half of the ROIs were randomly selected from the database of 80 ROIs. These ROIs were used to train the convolution neural network. The other half of the ROIs were then used to test the performance of the CNN. By choosing different random samples from the database, the jackknife test can be repeated to generate multiple test output and provide a better estimate of the true performance of the CNN in classifying benign and malignant clusters of microcalcifications.

ROC Analysis

The output values from the two output units were examined by using Receiver Operating Characteristic (ROC) analysis.[52,53] The LABROC4 algorithm[54] developed by Metz *et al.* was used to fit ROC curves to the continuous data from the output of CNN. The area under the ROC curve (A_z) was used as an overall measure of diagnostic performance. The result from each jackknife test was analyzed individually by using ROC analysis. Ten jackknife tests were performed. A final ROC curve was obtained by averaging the results from the 10 jackknife tests, as shown in Figure 8. The CNN system performed very well in classifying benign and malignant clusters of microcalcifications, achieving an A_z value of 0.90.

Potential Application in Recommending Courses of Action

A potential application of CNN is to classify microcalcifications into groups of definitely benign and possibly malignant. By applying a low threshold level to the output values of the CNN, we can make CNN a classifier that is not very specific but with 100% sensitivity.

With such a classifier, some benign microcalcifications may be classified as possibly malignant, but all of the microcalcifications classified as benign are definitely negative. Thus, radiologists can ignore the clusters of microcalcifications that are classified as benign and only concentrate on those that are classified as possibly malignant. As a result, the time radiologists spend reading mammograms can be reduced and detection efficacy of breast cancer can be expected to improve.
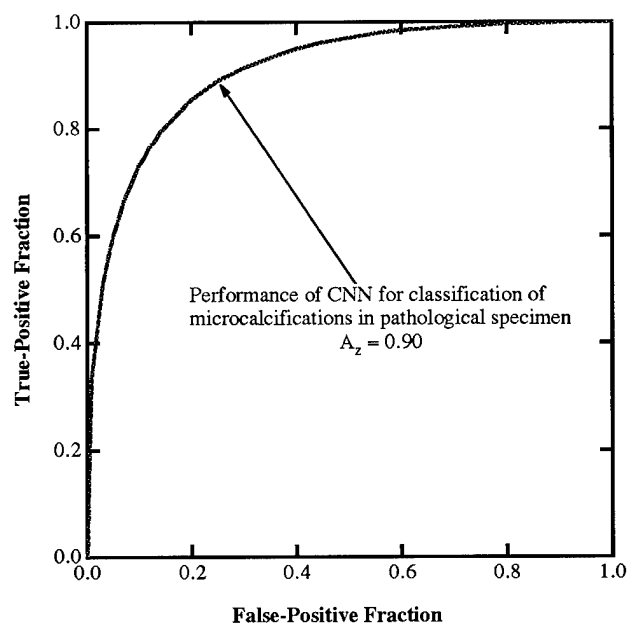
Figure 8   ROC analysis of the performance of CNN in classifying benign and malignant
            microcalcifications.

The ability of CNN to serve as a classifier to eliminate benign microcalcifications can be
demonstrated in Table I. In each of the jackknife tests, we set threshold levels of the output
of CNN such that all of the malignant ROIs are to be called positive by the computer system
and calculate the number of the benign ROIs that can be called negative (i.e., have output
values below the threshold level for positive ROIs).

Table I shows the results for each individual jackknife test as well as the averaged results of
the 10 jackknife tests (second column). The CNN can identify, on average, approximately
42% of the benign clusters of microcalcifications with 100% sensitivity (without missing any
malignant clusters). Therefore, if this CNN system were used to help radiologists in detecting
malignant microcalcifications, radiologists would only need to examine about half of the
detected microcalcifications.

As discussed earlier, studies have shown that approximately 10-30% of breast cancers are
missed by mammography and only 10-30% of biopsy cases recommended by mammography
are actually malignant. As a comparison to the reported performance of radiologists in breast
cancer diagnosis, we also listed in Table I (third and fourth columns) the average specificities
and positive predictive values, defined as the portion of malignant cases among the biopsied
cases.

With a sensitivity of 80%, approximately the same level of sensitivity reported by average radiologists, the neural network system achieved a positive predictive value for malignancy of 84%, compared with 10-30% achieved by radiologists. Therefore, the CNN appears to be a very promising tool for assisting radiologists in making decisions for the diagnosis of breast cancer.

Real mammograms

Genetic algorithms are employed to optimize the structure of a neural network and select the best performing subset from the initial image features. Additional cases of patients that have been recalled for further examination are being collected at GUMC. The performance of the neural network system based on these cases will help determining the usefulness of the system in reducing unnecessary biopsies.

Optimized Feature Set by Genetic Algorithms

Genetic Algorithms were applied to the first subset of seventy cases selected from the database. Two different sets of image features, each consisting of six features, were selected as a result of the optimization process. The neural network performed equally well with the two selected subsets.

Feature Set #1:
1. V3, size of the largest microcalcification in Image1
2. V4, size of average microcalcification in Image1
3. V5, size of smallest microcalcification in Image1
4. E1, ellipticity of the largest microcalcification on Image1
5. WAE, weighted average ellipticity of microcalcifications on Image1
6. A_x, length of semi-major axes of the fitted ellipse of a cluster on Image1

Feature Set #2:
1. E1, ellipticity of the largest microcalcification on Image1
2. WAE, weighted average ellipticity of microcalcifications on Image1
3. A_x, length of semi-major axes of the fitted ellipse of a cluster on Image1
4. B_x, length of semi-minor axes of the fitted ellipse of a cluster on Image1
5. V3 - V4
6. V4 - V5

The optimized parameters for the neural network are: learning rate 0.7 ~ 0.95 and momentum 0.02 ~ 0.06.

We evaluated the performance of the optimized neural network by using round-robin method and ROC analysis. Figure 9 shows the ROC curve for the classification of microcalcifications based on extracted image features.
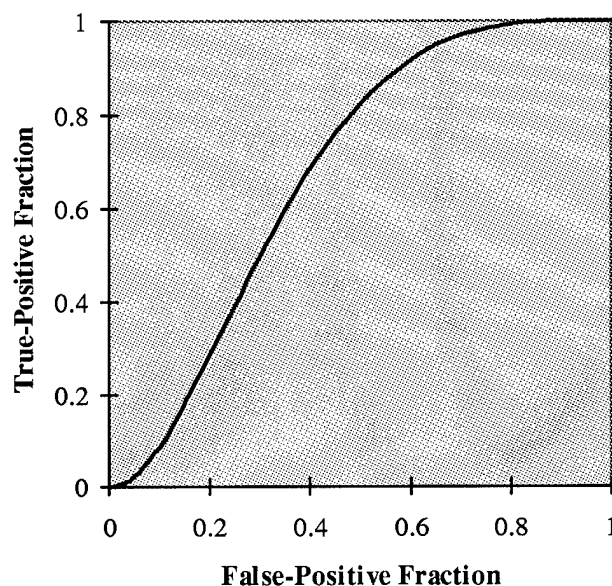

Figure 9 Performance of feature-based neural network in classification of microcalcifications

The system of neural network and genetic algorithms improved performance over our previous TRBF neural network[55]. The neural network system was able to classify benign and malignant microcalcifications at a level favorably compared to experienced radiologists. On the same database evaluated, the ROC curve for an experienced radiologist yielded an A_z of 0.54, while the A_z of the ROC curve for the neural network with optimized structure is 0.68. The use of the neural network system can be used to help radiologists reducing the number biopsies in clinical applications.

DISCUSSIONS

It is important to note that the CNN is designed as an automated classifier of microcalcifications for the diagnosis of breast cancer. It will be used in conjunction with other schemes for the detection of microcalcifications in digital mammograms. Once microcalcifications are detected, the CNN will be applied to classify them into benign (negative) and malignant (positive) groups. Radiologists can ignore the microcalcifications that are classified into the benign group and examine those that are classified as malignant to decide whether to recommend biopsy or short term follow-up exams.

Table I. Application of CNN in Recommending Courses of Action

Jackknife Test	Correctly identified negative cases at 100% sensitivity	False Positives at 90% sensitivity	False Positives at 80% sensitivity
1	16	2	2
2	12	7	2
3	15	2	0
4	2	6	6
5	11	3	1
6	4	2	2
7	7	4	2
8	7	8	8
9	3	5	5
10	6	5	2
Average	8.3	4.4	3
Average Specificity	42%	78%	85%
Positive Predictive Value*	63%	80%	84%

Positive Predictive Value — Defined as the portion of the actually positive cases among the cases diagnosed that are classified as positive by a diagnostic system.

The results discussed are based on radiographs of biopsy specimen of microcalcifications. The specimen images have, in general, better image quality and greater signal-to-noise ratio than the regular mammograms. The radiographs digitized with high resolution digitizers provide the morphological information of individual microcalcifications that makes the classification of microcalcifications into benign and malignant groups possible. The CNN system will need to be tested on regular mammograms. Some parameters of CNN may need to be fine tuned when applied to regular mammograms and the CNN system may not achieve the same performance level as it did in this study.

Both a large training and testing database are necessary in order to train and evaluate the performance of the neural network sufficiently and reliably. We will be expanding our database significantly in the future. To further improve the accuracy of the classification, a hybrid neural network (HNN)[56] will also be employed to classify microcalcifications based on the input of both image data and image features[57] that will be automatically extracted.

The evaluation of feature based neural network with Generic Algorithm was based on a very difficult data set which was different from what was used for evaluation of image based neural

networks. The microcalcification clusters in the data set for feature based neural network are very subtle and an experienced radiologist only scored an A_z of 0.54 in classifying between benign and malignant clusters. The size of the database is also small. We are currently in the process of expanding our database to include more mammograms from different hospitals.

Conclusions

We have demonstrated that the convolution neural networks can be an effective tool in the diagnosis of breast cancer. The results obtained in this study are very promising, even though they were based on a relatively small training and testing database. These results indicate the potential usefulness of CNN in classification of microcalcifications in digital mammograms. An extensive clinical test of our developed system using real mammograms will be needed to determine the clinical applicability.

Genetic algorithms are an effective tool to select optimal input features and structure of a backpropagation neural network. The neural network, combined with genetic algorithms, is able to effectively classify benign and malignant microcalcifications. The results of the neural network system can be used to help reducing the number of benign biopsies.

References

1. American Cancer Society. Mammography 1982: A statement of the American Cancer Society. CA Cancer J. Clin. **1982**; 32: 226-230.

2. Lester RG. The contribution of radiology to the diagnosis, management, and care of breast cancer. Radiology **1984**; 151: 1-7.

3. Kopans DB, Mayer JE, Sadowsky N. Medical progress: Breast imaging. N. Engl. J. Med **1984**; 310: 960-967.

4. Millis RR, Davis R, Stacey AJ. The detection and significance of calcifications in the breast: A radiological and pathological study. Br. J. Radiol **1976**; 49: 12-26.

5. American Cancer Society. Mammography guidelines 1983: Background statement and update of cancer related checkup guidelines for breast cancer detection in asymptomatic women age 40 to 49. CA Cancer J. Clin **1983**; 33: 255.

6. Baker LH. Breast cancer detection demonstration project: Five-year summary report. CA Cancer J. Clin **1982**; 32: 194-225.

7. NCRP Report No. 85. Mammography — A User's Guide (National Council on Radiation Protection and Measurement). Washington, DC; **1986**.

8. Feig SA. Decreased breast cancer mortality through mammographic screening: results of clinical trials. Radiology **1988**; 167: 659-665.

9. Hall FM, Storella JM, Silverstone DZ, Wyshak G. Nonpalpable breast lesions: Recommendations for biopsy based on suspicion of carcinoma at mammography. Radiology **1988**; 167: 353-358.

10. Bassett LW, Gold RH. Breast Cancer Detection: Mammography and Other Methods in Breast Imaging. New York: Grune & Stratton; **1987**.

11. Baines CJ, Miller AB, Wall C, et al. Sensitivity and specificity of first screen mammography in the Canadian National Breast Screening Study: A preliminary report from five centers. Radiology **1986**; 295-298.

12. Pollei SR, Mettler FA, Bartow SA, Moradian G, Moskowitz M. Occult breast cancer: prevalence and radiographic detectability. Radiology **1987**; 163: 459-462.

13. Anderson I. What can we learn from interval carcinomas? Recent Results Cancer Res **1984**; 90: 161-163.

14. Martin JE, Moskowitz M, Milbrath JR. Breast cancer missed by mammography. AJR **1979**; 132: 737-739.

15. Vernon MD. The Psychology of Perception. Middlesex, England: Penguin; **1962**.

16. Tuddenham WJ. Visual search, image organization and reader error in roentgen diagnosis. Radiology **1962**; 78: 694-704.

17. Smith MJ. Error and Variation in Diagnostic Radiology. Springfield, IL: Charles C. Thomas Publisher; **1967**.

18. Lehr JL, Lodwick GS, Farrel C, Braaten MO, Virtama P, Koivisto EL. Direct measurement of the effect of film miniaturization on diagnostic accuracy. Radiology **1976**; 118: 257-263.

19. Hillman BJ, Fajardo LL, Hunter TB, al. e. Mammogram interpretation by physician asistants. AJR **1987**; 149: 907-911.

20. Sickles EA. Mammographic detectability of breast microcalcifications. AJR **1982**; 139: 913-918.

21. Wolfe JN. Analysis of 462 carcinomas. AJR **1974**; 121: 846-853.

22. Murphy WA, DeSchryver-Kecskemeti K. Isolated clustered calcifications in the breast: Radiologic-pathologic correlation. Radiology **1978**; 127: 335-341.

23. Fisher ER, Gregorio RM, Fisher B, Redmond C, Vellios F, Sommers SC. The pathology of invasive breast cancer. Cancer **1975**; 36: 1-85.

24. Black JW, Young B. A radiological and pathological study of the incidence of calcifications in diseases of the breast and neoplasms of other tissue. Br. J. Radiol **1965**; 38: 596-598.

25. Lanyi M. Diagnosis and Differential Diagnosis of Breast Calcifications. Berlin, Heidelberg: Springer-Verlag; **1988**.

26. Stomper P, Connolly JL, Meyer JE, Harris JR. Clinically occult ductal carcinoma in situ detected with mammography. Radiology **1989**; 172: 235-241.

27. Homer MJ, Cooper AG, Pile-Spellman ER. Milk of calcium in breast microcysts: manifestation as a solitary focal disease. Am. J. Radiol **1988**; 150: 78-79.

28. Egan RL, McSweeney MB, Sewell CW. Intramammary calcifications without an associated mass in benign and malignant diseases. Radiology **1980**; 137: 1-7.

29. Roses DF, Mitnick J, Harris MH, et al. The risk of carcinoma in wire localization biopsies for mammographically detected clustered microcalcifications. Surgery **1991**; 110: 877-886.

30. Dido F, Crowe J, Zollinger R, al. e. Biopsy of the breast for mammographically detected lesions. Surgery Gynecology and Obstetrics **1990**; 171: 449-455.

31. Leviathan LH, Within DM, Harrison EG. Calcification in breast disease: mammographic-pathologic correlation. AJR **1964**; 2: 29-39.

32. Freundlich IM, Hunter TB, Seeley GW, al. e. Computer assisted analysis of mammographic clustered microcalcifications. Clinical Radiology **1989**; 40: 295-298.

33. Chan H-P, Doi K, Galhotra S, Vyborny CJ, MacMahon H, Jokich PM. Image feature analysis and computer-aided diagnosis in digital radiography. 1. Automated detection of microcalcifications in mammography. Med Phys **1987**; 14: 538.

34. Chan H-P, Doi K, Vyborny CJ, Lam KL, Schmidt RA. Computer-aided detection of microcalcifications in mammograms: Methodology and preliminary clinical study. Invest Radiol **1988**; 23: 664.

35. Fam BW, Olson SL, Winter PF, Scholz FJ. Algorithm for the detection of fine clustered calcifications on film mammograms. Radiology **1988**; 169: 333.

36. Davies DH, Dance DR. Automatic computer detection of clustered calcifications in digital mammograms. Phys Med Biol **1990**; 35: 1111.

37. Chan H-P, Doi K, Vyborny CJ, Schmidt RA, Metz CE, Lam K-L, Ogura T, Wu Y, MacMahon H. Improvement in radiologists' detection of clustered microcalcifications on mammograms: The potential of computer-aided diagnosis. Invest Radiol **1990**; 25: 1102-1110.

38. Wu Y, Doi K, Giger ML, Nishikawa RM. Computerized detection of clustered microcalcifications in digital mammograms: Applications of artificial neural networks. Med Phys **1992**; 19: 555-560.

39. Nishikawa RM, Giger ML, Doi K, Vyborny CJ, Schmidt RA. Computer-aided detection of clustered microcalcifications using digital mammograms. Med. Bio. Eng. Com. **1994**; accepted for publication:

40. Astley S, Taylor C, Boggis C, Wilson M, Ellison T. Automated detection of microcalcifications in mammograms. Radiology **1990**; 177(P): 288.

41. Grimaud M, Muller S, Meyer F. Automated detection of microcalcifications in mammograms. Radiology **1990**; 177(P): 288.

42. Karssemeijer N. A stochastic method for automated detection of microcalcifications in digital mammograms. In: Colchester ACF, Hawkes DJ, eds. Information processing in medical imaging. New York: Springer-Verlag; **1991**: 227-238.

43. Hecht-Nielsen R. Neurocomputing. Reading, MA: Addison-Wesley Publishing Company; **1990**.

44. Grossberg S. Neural Networks and Neural Intelligence. Cambridge, MA: MIT; **1988**.

45. Anderson JA, Rosefeld E. Neurocomputing: Foundations of Research. Cambridge, MA: MIT; **1988.**

46. Fukushima K, Miyake K, Ito T. Neocognitron: A neural network model for mechanism of visual pattern recognition. IEEE Transactions of Systems, Man, and Cybernetics **1983**; 13: 826-834.

47. Lo S-CB, Lin J-S, Freedman MT, Mun SK. Computer-assisted diagnosis of lung nodule detection using artificial convolution neural network. SPIE Medical Imaging 1993 Image Processing 1993, 1898: 859-869. Newport Beach, CA.

48. Zhang W, Hasegawa A, Itoh K, Ichioka Y. Image processing of human corneal endothelium based on a learning network. Appl. Opt. **1991**; 30: 4211-4217.

49. Hasegawa A, Zhang W, Itoh K, Ichioka Y. Neural Network-based Image Processing on Human Corneal Endothelial Micrograms. Proc. SPIE 1991, 1558: 414-421.

50. Fukushima K, Miyake S. Neocognitron: A New Algorithm for Pattern Recognition Tolerant of Deformations and Shift in Position. Pattern Recognition **1982**; 15: 455-469.

51. Rumelhart DE, McClellend JL. Parallel Distributed Processing: Explorations in the Microstructure of Cognition. Cambridge, MA: MIT Press; **1986.**

52. Metz CE. ROC methodology in radiologic imaging. Invest Radiol **1986**; 21: 720-733.

53. Metz CE. Basic principles of ROC analysis. Seminars in Nuclear Medicine **1978**; VIII: 283-298.

54. Metz CE, Shen J-H, Herman BA. New methods for estimating a binormal ROC curve from continuously-distributed test results. 1990 Joint Meetings of the American Statistical Society and the Biometric Society 1990, Anaheim, CA.

55. Tsujii O, Hasegawa A, Wu CY, Lo S-C, Freedman MT, Mun SK. Classification of Microcalcifications in Digital Mammograms for the Diagnosis of Breast Cancer. SPIE Medical Imaging 1996, 2710: 794-804. Newport Beach, CA.

56. Wu YC, Lo S-CB, Freedman MT, Mun SK. Automatic detection of lung nodules with used of parametric and nonparametric neural networks. Radiology **1992**; 189 (P): 272.

57. Wu Y, Giger ML, Doi K, Vyborny CJ, Schmidt RA, Metz CE. Artificial neural networks in mammography: Application to decision making in the diagnosis of breast cancer. Radiology **1993**; 187: 81-87.

Appendix

Publications supported under current grant

1. Wu YC, Freedman MT, Hasegawa A, Zuurbier RA, Lo S-CB, Mun SK. Classification of microcalcifications in the radiographs of pathological specimen for the diagnosis of breast cancer. Academic Radiology **1995**; 2: 199-204.

2. Wu CY, Hasegawa A, Freedman M, Zuurbier R, Mun SK. CADx in Digital Mammography: Classification of Microcalcifications for Diagnosis of Breast Cancer. International Symposium on Computer and Communication Systems for Image Guided Diagnostics and Therapy 1995, 352-356. Berlin, Germany.

3. Wu CY, Patt RH, Freedman MT, Mun SK. Diagnosis of breast cancer by MRI: A 3D computer visualization and analysis system. SPIE Medical Imaging 1996 —Image Display 1996, 2707: 87-96. Newport Beach, California.

4. Wu CY, Freedman MT, Hasegawa A, Mun SK. Quality Control in Digital Mammography: Automatic Detection of Under and Over-Exposed Mammograms. SPIE Medical Imaging 1997 — Image Perception 1997, Newport Beach, California.

5. Wu CY, Tsujii O, Freedman MT, Mun SK. Image Feature Analysis for Classification of Microcalcifications in Digital Mammography: Neural Networks and Genetic Algorithms. SPIE Medical Imaging 1997 — Image Processing 1997, Newport Beach, California.